

An investigation into the mechanism of nobiletin's inhibition of papillary thyroid cancer using network pharmacology analysis and experimental pharmacology

Q.-J. DU¹, Q. LI², R.-H. ZHOU³, H. WANG³, Q. YAN³, W.-J. DANG¹, J.-J. GUO¹

¹Third Hospital of Shanxi Medical University, Shanxi Bethune Hospital, Shanxi Academy of Medical Sciences, Tongji Shanxi Hospital, Taiyuan, China

²Shanxi Medical University, Jinzhong, China

³Second Clinical Medical College, Shanxi Medical University, Taiyuan, China

Qiuqing Du and Qian Li have contributed equally to this work and share the first authorship

Abstract. – OBJECTIVE: Surgery and radioactive iodine therapy are the main treatments for papillary thyroid carcinoma (PTC), and effective drugs are lacking. As a promising natural product, nobiletin (NOB) has a wealth of pharmacological activities like anti-tumor, antiviral, and other effects. In this research, bioinformatics methods and cellular assays were combined to explore how NOB inhibited PTC.

MATERIALS AND METHODS: Our NOB targets were derived from three databases, including the SwissTargetPrediction database, Traditional Chinese Medicine System Pharmacology Database, and the TargetNet server. Four databases were used to identify disease-related targets: GeneCards, PharmGkb, Online Mendelian Inheritance in Man, and DisGeNET. Finally, cross-targets of disease and drug were deemed as pharmacological targets, and they were used for GO and KEGG enrichment analysis. STRING and Cytoscape were applied for PPI Network and core Targets Ranking. Molecular docking analysis validated binding affinity values for NOB and core targets. By using cell proliferation and migration assays, NOB was assessed for its effects on PTC proliferation and migration phenotype. Western blot validated the downregulation of the PI3K/Akt pathway.

RESULTS: (1) Preliminarily, 85 NOB targets were predicted for NOB intervention in PTC. (2) Our core target screening identified *TNF*, *TP53*, and *EGFR*, and our molecular docking results confirmed good binding between NOB and protein receptors. (3) NOB inhibited proliferation and migration of PTC cells. PI3K/AKT pathway target proteins were downregulated.

CONCLUSIONS: (1) Bioinformatics analyses revealed that NOB may inhibit PTC by regulating *TNF*, *TP53*, *EGFR* and PI3K/AKT signalling pathway. (2) As evidenced by cell experiments,

there was an inhibition of proliferating and migrating PTCs by NOB via the PI3K/AKT signalling pathway.

Key Words:

Nobiletin, Papillary thyroid carcinoma, Network pharmacology, Molecular docking.

Introduction

The incidence of thyroid carcinoma is rising worldwide¹. Differentiated thyroid cancer (DTC) accounts for 90% of thyroid cancers and most of them are papillary thyroid carcinomas (PTCs)². There has been an increase in the diagnosis of DTCs and PTCs, which are the main causes of the rise in incidence rates. While thyroid cancer incidence rates have remained relatively stable over the past 30 years for follicular, anaplastic, and medullary types³. The thyroid cancer mortality rate is relatively inert, increasing by 1.1% per year, but the poor prognosis that the rising mortality represents cannot be ignored⁴. Thyroid cancer mortality increased mainly due to advanced-stage PTC⁵. Approximately five to ten per cent of DTC patients will develop metastatic disease, usually affecting the lungs and bones, and two-thirds of these patients will become RAI-refractory DTC⁶, who lose the ability to absorb iodine little by little as a result of de-differentiation and have a poor prognosis with an average lifespan of only three to five years⁷. Therefore, PTC requires a deeper understanding of its mechanisms and novel therapeutic approaches.

A total of 49% of FDA new drug approvals from 1981 to 2014 were based on natural products or derivatives of a natural product pharmacophore⁸. In addition to their structural diversity, natural products have diverse biologic activities, low toxicity, and they are available from a variety of sources⁹. The flavonoid nobiletin (NOB) can be obtained in citrus peel and is an active ingredient in traditional Chinese medicine such as *Centipedeae Herba*, *Citrus Reticulata*, *Tripterygii Radix*¹⁰, which has a wealth of pharmacological activities like antitumor, antiviral, anti-inflammatory, antioxidant, and antidiabetic effects^{11,12}. We were pleasantly surprised by its anticancer activity in various tumors, like lung cancer¹³, renal carcinoma¹⁴, and ovarian cancer¹⁵. Furthermore, in normal tissues and cancer cells, nobiletin may have a dual role, which means that it may increase the sensitivity of cancer cells to anticancer drugs in addition to protecting normal tissues, just like the characteristics of other herbal-derived agents¹⁶. Research has shown that multi-drug resistance can be reversed by nobiletin safely and efficiently¹⁷. In brief, considerable reports have indicated that this is a promising natural product.

Network pharmacology integrates systems biology, molecular biology, pharmacology, and other emerging macro-to-micro disciplines¹⁸. Com-

puter-aided drug design relies heavily on molecular docking to predict protein-ligand binding affinity¹⁹. For the first time, we have discovered and reported that tangeretin, an antioxidant derived from citrus peel, can enhance insulin sensitivity in the liver by suppressing the MEK-ERK1/2 pathway²⁰. Based on interest in flavonoids derived from citrus and their demonstrated therapeutic potential, we predicted the core targets and key signalling pathways of NOB intervention in PTC through network pharmacology, molecular docking, and other bioinformatics methods. In cell experiments, we demonstrated that NOB inhibited the proliferation and migration of PTC cells through PI3K/AKT pathway. The design idea of our project was shown in Figure 1. When current standard treatments fail to achieve good results, bringing more treatment options to patients, including more therapeutic targets and more economical and convenient drugs, has become the direction of our research.

Materials and Methods

Data Collection and Target Prediction

To clarify the effective targets of NOB, we obtained NOB targets from three databases, in-

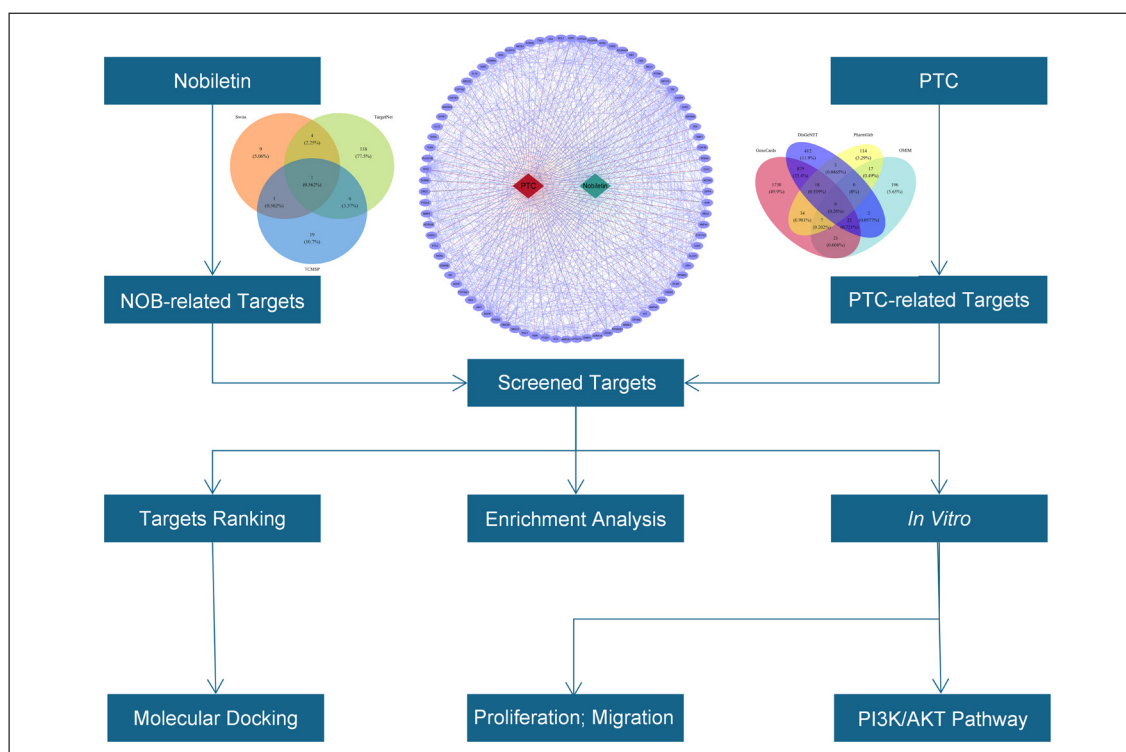


Figure 1. A flow chart describes the design of a team project.

cluding the SwissTargetPrediction database²¹, Traditional Chinese Medicine System Pharmacology Database (TCMSP), and the TargetNet web server²². Disease-related targets were associated with 4 databases, which were comprised of GeneCards²³, PharmGkb²⁴, Online Mendelian Inheritance in Man (OMIM)²⁵, and DisGeNET²⁶. Finally, cross-targets of disease and drug were deemed as pharmacological targets.

Further Exploration of the Screened Targets

With the application of DAVID Bioinformatics Resources²⁷, we further performed further enrichment analysis on the screened targets, which were targets of NOB intervention in PTC. The objective of Gene Ontology (GO) enrichment analysis was to explore the function of pharmacological targets, containing biological process (BP), molecular function (MF), and cellular compartment (CC). Meanwhile, we could be acquainted with the signalling pathways involved in the targets, under the Kyoto Encyclopedia of Genes and Genomes (KEGG) pathway analysis. We mapped the possible transduction of the PI3K-AKT pathway in combination with predicted targets.

Establishment of Protein-Protein Interaction (PPI) Network and Pharmacological Targets Ranking

The screened targets were imported into STRING (version 11.5; <https://string-db.org/>) to establish a PPI network, which gave a summary of the network about anticipated interconnections for screened proteins. With the application of CytoHubba from Cytoscape (version 3.9.0)²⁸, we could predict and seek crucial nodes and weak parts in an interactome network by our chosen topological algorithms, which consisted of Degree, Maximum Neighborhood Component (MNC), Maximal Clique Centrality (MCC), Closeness, Edge Percolated Component (EPC) and Betweenness.

Molecular Docking

We downloaded crystal structures of proteins from the RCSB Protein Data Bank (PDB) database²⁹⁻³¹, and we obtained the small molecule ligand structure from PubChem. DeepSite³² is based on deep neural networks and can predict protein binding pockets. With the upload of PDB files, the application of DeepSite helps us predict the position of druggable binding sites

very well. AutoDock Vina 1.2.3³³ was used for molecular docking studies. PLIP³⁴ and PyMOL³⁵ were used to analyze and visualize non-covalent interactions between biomacromolecules and their ligands.

Cultivation of the PTC Cell Line

Chinese Academy of Sciences Cell Bank provided the B-CPAP cell line (PTC cell line). The mycoplasma test result of the cell line was negative, and the STR test was correct. B-CPAP Cells were nurtured in RPMI-1640 medium mixed with 10% fetal bovine serum, in 5% carbon dioxide, at 37°C.

Nobiletin IC50 and Cell Proliferation

CCK-8 assay (Boster, China) was used to assess the proliferative impact of NOB (HY-N0155, MCE) at different concentrations. For 24 hours, the cells were cultivated on 96-well plates (3,000/well) under appropriate culture conditions. Then different concentrations of NOB (40 μ M, 80 μ M, 120 μ M) and DMSO (0.8%, 1.6%, 2.4%) were added respectively. After 24 hours, the medium was removed, and the CCK-8 reaction solution (10% culture system) was put on plates according to the manufacturer's instructions. We measured the absorbance at 450 nm after incubation for 1-4 hours and then calculated the NOB IC50 using GraphPad Prism software (La Jolla, CA, USA).

Wound Healing

Cells were sowed in six-well plates (2×10^5 cells/well). When cells came up to 90% confluence, we made an equal-width scratch in the plate with a 200 μ L pipette tip and washed it three times with PBS intending to remove scraped cells. Then wells were grouped into drug (30 μ L and 60 μ L NOB) and control group (0 μ L NOB), and incubated for 24 hours, maintaining with serum-free medium. Scratch healing was observed at 0 h and 24 h, while we chose 5 fields of view to take pictures through the microscope in each well. With the percentage of relative wound closure assessed, we contemplated differences in cell migration that were shown in drug groups by contrast with the control group.

Western Blotting

With the usage of RIPA lysis buffer (Boster, China) supplemented with protease inhibitors and phosphatase inhibitors (Keygen, China), we lysed different groups of cells on ice. Cell lysates were picked up and centrifuged at 10,000 g for 10

minutes. Quantifying protein concentrations was done using a BCA protein assay kit (Boster, China). Electrophoresis was used to separate samples with equal amounts of protein. Proteins were transferred to nitrocellulose membranes (Boster, China), and 5% nonfat milk was used to block nitrocellulose membranes for 1 hour at room temperature before blocking with primary antibodies overnight at 4°C. The primary antibodies were as follows: *PI3KCA* (A0265, 1:1000, Abclonal, China), P-PI3K p85 (Tyr458)/p55 (Tyr199) (#4228, 1:1000, CST, USA), *AKT1* (A17909, 1:1000, Abclonal, China), P-AKT (AP0140, 1:1000, Abclonal, China), *GAPDH* (ab181602, 1:3000, Abcam, UK). Incubation with secondary antibodies was performed after washing the membranes three times with Tris-buffered saline containing Tween-20 (0.1%). Finally, membranes were treated with a chemiluminescent reagent and exposed to X-rays.

Statistical Analysis

The following software were utilized for data extraction and analysis: R software (version 4.1.0), Strawberry Perl software (version 5.30.1-64bit), GraphPad Prism software (version 8.0.2; La Jolla, CA, USA) and SPSS software v.26.0 (IBM, Armonk, NY, USA). In *in vitro* studies, paired *t*-test was used for variance analysis of two-sample means; One-way ANOVA was used for overall variance analysis of multi-sample means; Turkey and Dunnett-*t* statistical methods were used for pairwise comparison of multi-sample means. A description of the significance of the *p*-value: ns means $p > 0.05$ (not significant); *

means $0.01 < p < 0.05$; ** means $0.001 < p < 0.01$; *** means $p < 0.001$.

Results

Determination of NOB Targets Against PTC

Referring to drug-related targets, 15 targets, 35 targets, and 153 targets were derived from SwissTargetPrediction, TCMSP and TargetNet, respectively (Figure 2A). With the filter criteria of relevance score greater than 1, we screened 2,723 targets from the 2,773 PTC disease-related targets in GeneCards. The final collection of disease-related targets was finished after we obtained 202 targets from PharmGkb, 287 targets from OMIM, and 1348 targets from DisGeNET (Figure 2B). With duplicate targets among databases removed, 85 NOB targets for intervention in PTC were preliminarily predicted (Figure 3).

Further Exploration of Initially Predicted Targets

In GO enrichment analysis, biological processes mainly referred to signal transduction, negative regulation of cell proliferation, inflammatory response and so on (Figure 4). With the consequences of the KEGG enrichment analysis, the signalling pathways of NOB intervention in PTC were mainly focused on the pathways in cancer, PI3K/AKT signalling

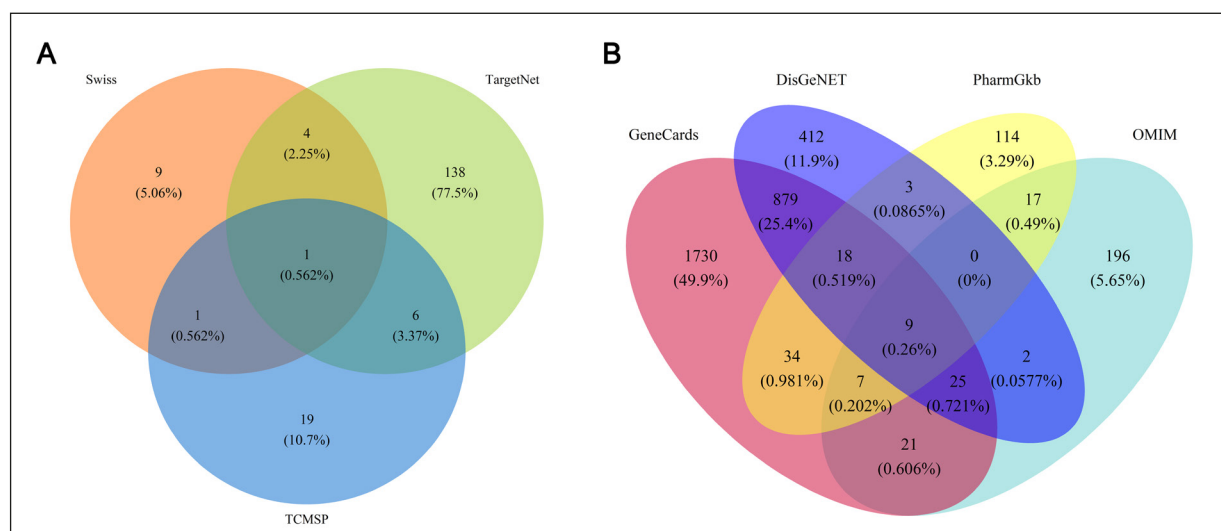


Figure 2. A, The distribution of NOB-related targets. B, The distribution of PTC-related targets.

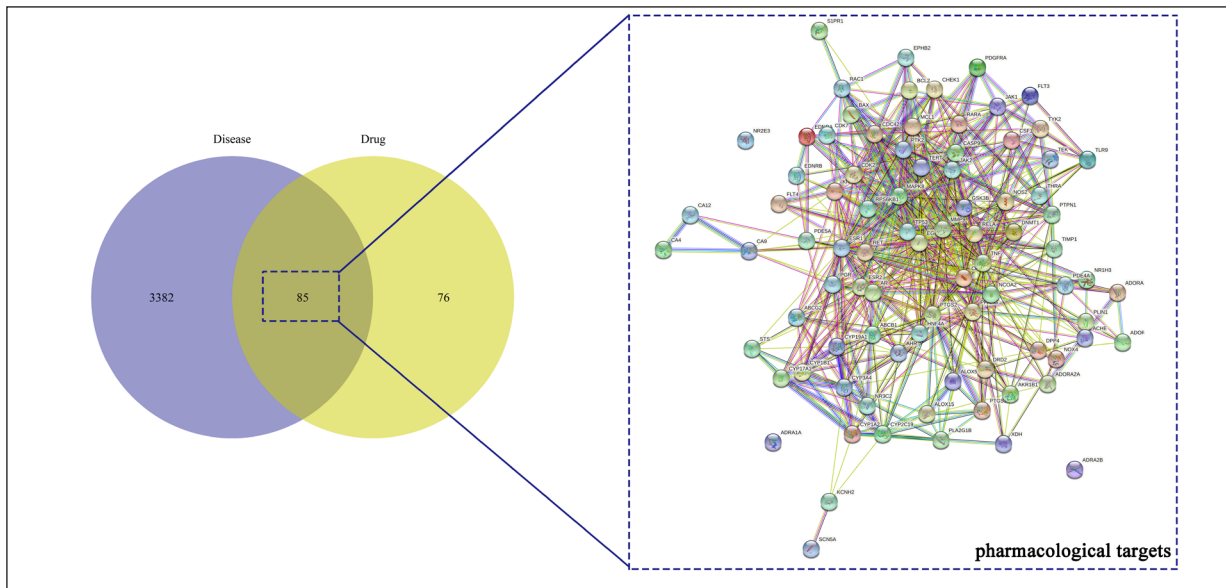


Figure 3. The Venn diagram of NOB and PTC targets. The PPI network map of protein interactions was derived from STRING.

pathway, chemical carcinogenesis-receptor activation, prostate cancer, pancreatic cancer (Figure 4). Combined with predicted targets, the PI3K/AKT pathway was depicted in Figure 5 with the application of ScienceSlides.

The PPI of NOB Targets against PTC and Pharmacological Targets Ranking

With the implementation of STRING and Cytoscape, a processed network based on the PPI network not only demonstrated the interaction

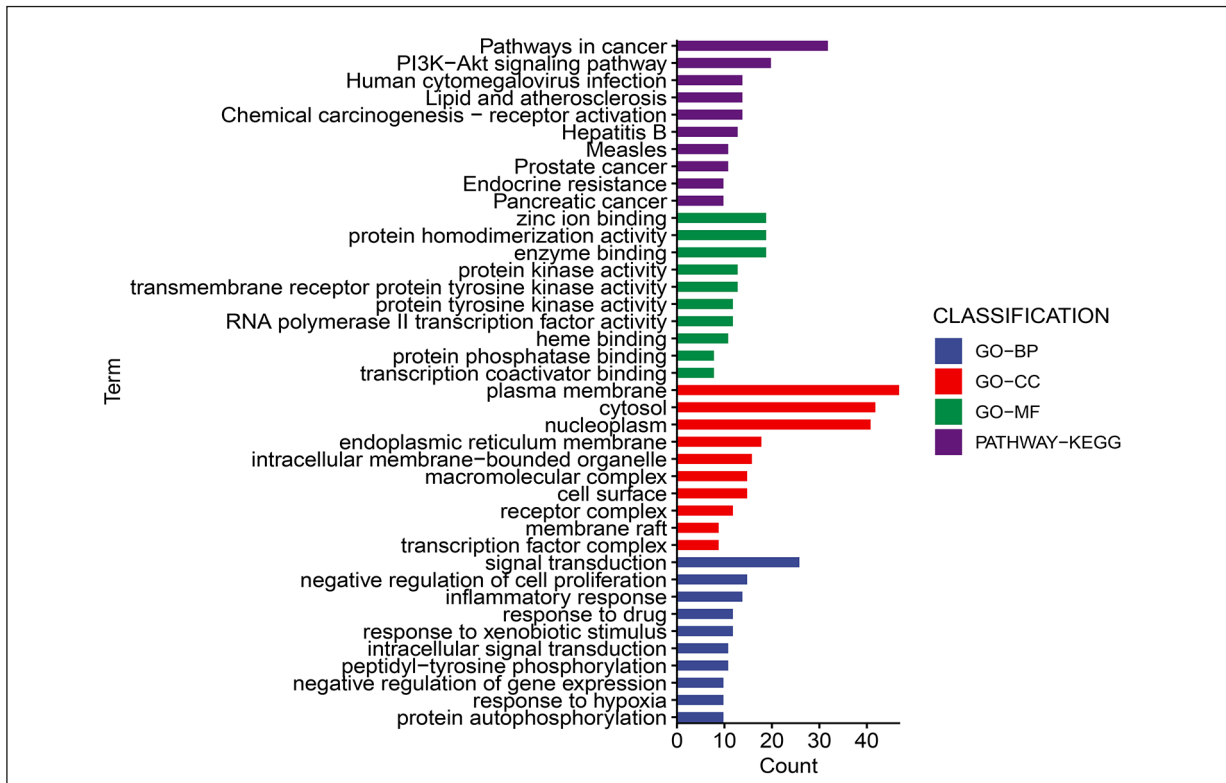


Figure 4. GO and KEGG enrichment analysis based on 85 potential targets.

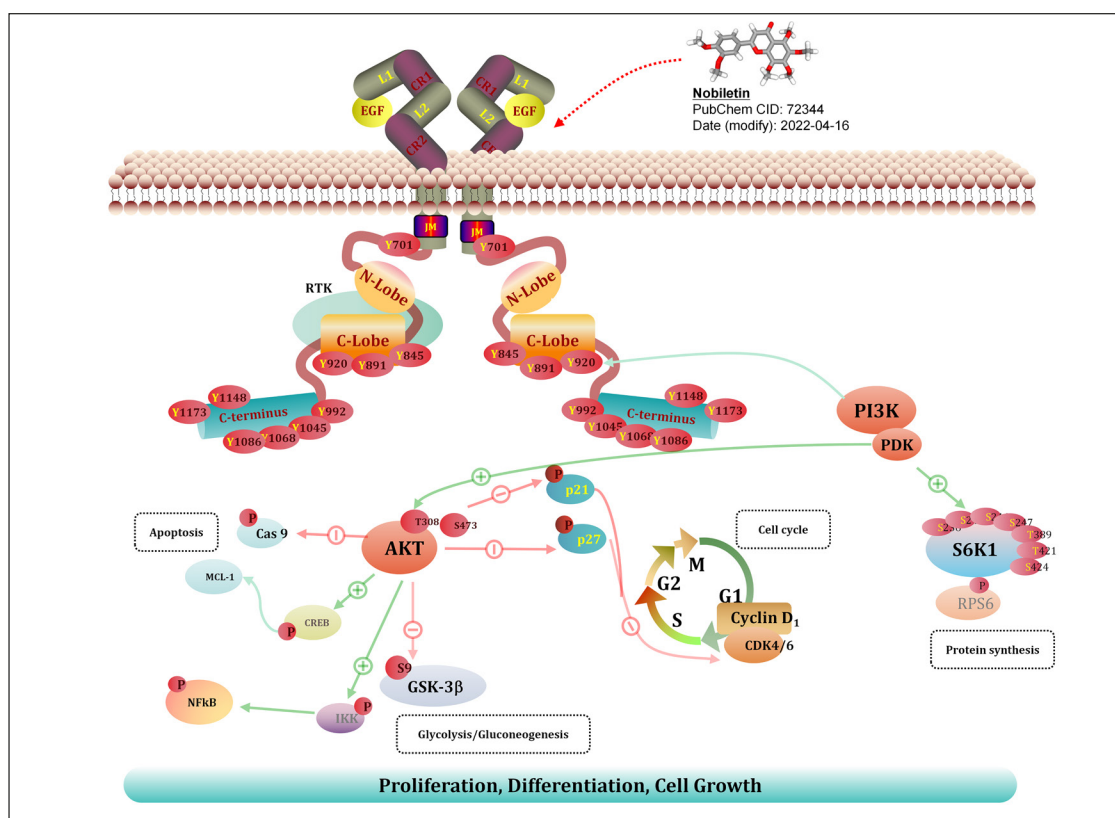


Figure 5. Display of PI3K/AKT signaling pathway possibly mediated by NOB based on bioinformatics analysis results.

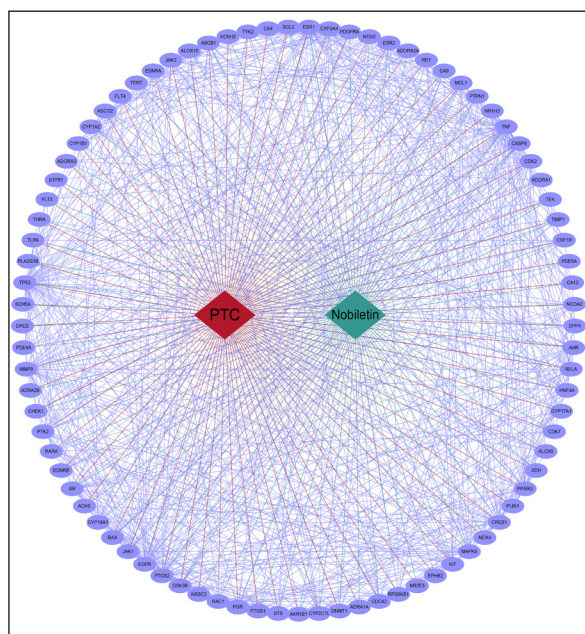


Figure 6. A processed network with the implement of STRING and Cytoscape. Red lines connect PTC and its associated targets, and green lines connect NOB and its associated targets.

among pharmacological targets, but also indicated the connection among NOB, PTC, and pharmacological targets (Figure 6). *Via* our chosen topological algorithms in CytoHubba, we got the top fifteen rankings of targets in different algorithms (Table I). Based on the top three most consistent results shown by various algorithms, we selected *TNF*, *TP53* and *EGFR* for molecular docking with NOB to assess their binding activities.

Molecular Docking Analysis

It is recognized that binding affinity values lower than -5.0 kcal/mol indicate good interactions, and binding is stronger at a lower number³⁶. The good binding of NOB and protein receptors verified the calculation results obtained by the CytoHubba algorithm. This suggested that NOB may inhibit PTC by interfering with the core targets of *TNF*, *TP53* and *EGFR*. Docking results for the NOB ligand and core target protein receptors were depicted in Table II and Figure 7.

NOB Reduced PTC Proliferation and Migration

The 24h IC₅₀ value of NOB was 57.85 μ M for the B-CPAP cell line (Figure 8A). By further

Table I. Pharmacological Targets Ranking based on different algorithms.

Category	Rank Methods in CytoHubba					
	Degree	MCC	MNC	EPC	Closeness	Betweenness
1	TNF	TP53	TNF	TP53	TNF	TNF
2	TP53	TNF	TP53	TNF	TP53	TP53
3	EGFR	CREB1	EGFR	ESR1	EGFR	ESR1
4	ESR1	PTGS2	ESR1	EGFR	ESR1	EGFR
5	CREB1	EGFR	CREB1	MMP9	PTGS2	CREB1
6	PTGS2	ESR1	PTGS2	PTGS2	MMP9	PPARG
7	MMP9	MMP9	MMP9	MAPK8	CREB1	CYP3A4
8	PPARG	RELA	PPARG	CREB1	PPARG	PTGS2
9	MAPK8	CASP9	MAPK8	PPARG	MAPK8	MMP9
10	RELA	MAPK8	RELA	RELA	RELA	KCNH2
11	AR	MCL1	AR	MCL1	AR	CA9
12	MCL1	AR	MCL1	AR	MCL1	AR
13	JAK2	PGR	JAK2	JAK2	KIT	CYP1A2
14	KIT	JAK2	KIT	KIT	PGR	MAPK8
15	PGR	PPARG	PGR	GSK3B	JAK2	RELA

Table II. Binding affinity values (kcal/mol) of nobiletin and the core targets based on molecular docking.

Receptor ligand	TNF	TP53	EGFR
Nobiletin	-7.68	-8.36	-7.01

analysis, we found that the viability of cells treated with 40 μM and 60 μM NOB was inhibited significantly compared with the respective experimental controls (DMSO controls), in a concentration-de-

pendent manner (Figure 8B). Contrasted with the blank control (no drug added), the viability of cells treated with 40 μM , 60 μM , and 80 μM NOB was inhibited significantly, in a concentration-depen-

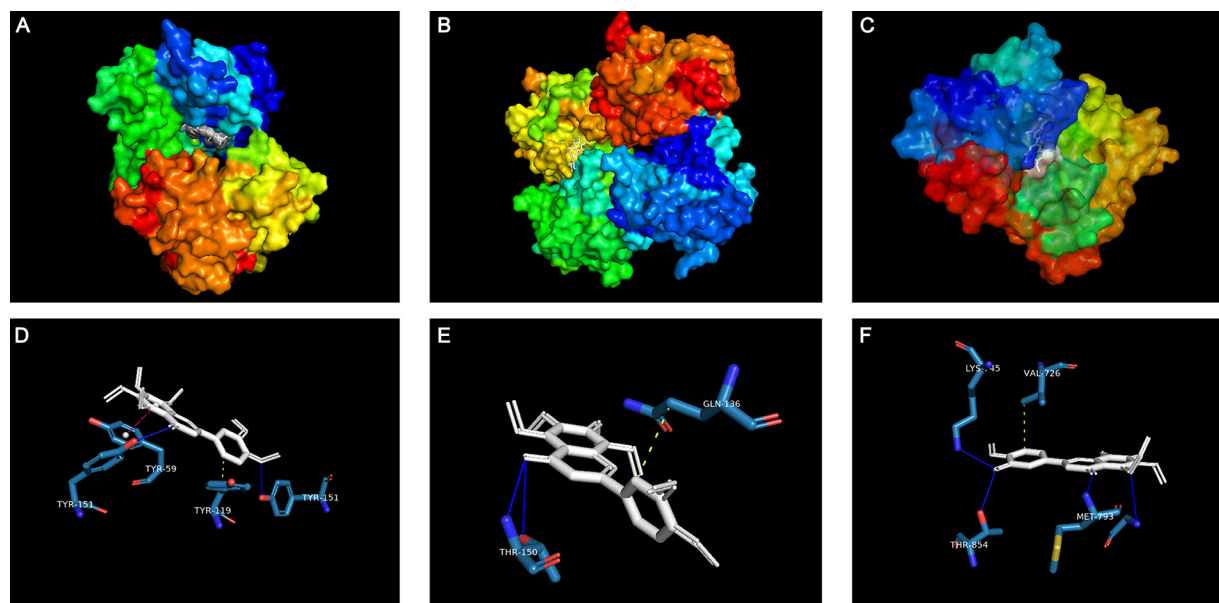


Figure 7. Docking results for the NOB ligand and core target protein receptors. The global molecular docking results of *TNF*, *TP53*, and *EGFR* were depicted in Figures A-C, respectively, while the local interactions were depicted in Figures D-F. The line colors that represent interactions are configured as follows: Hotpink lines represent π -stacking (parallel); Limon lines represent hydrophobic interactions; Blue lines represent hydrogen bond. The ligand NOB is highlighted with white sticks in all pictures.

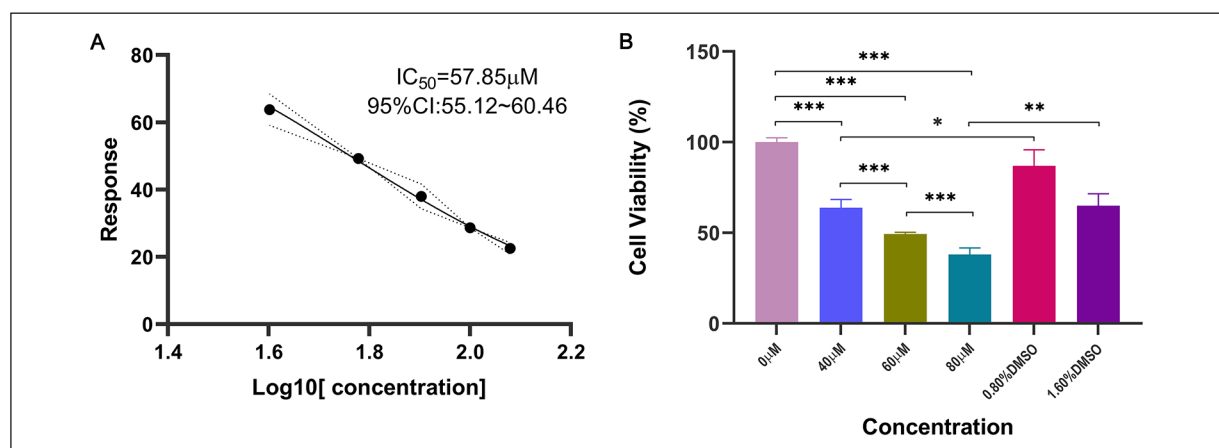


Figure 8. In PTC cells, NOB reduced cell proliferation. **A**, The dose-effect curve of NOB on B-CPAP cells for 24 h. **B**, Statistical analyses of cell viability differences among NOB experimental groups and control groups.

dent manner. B-CPAP cells were exposed to NOB (30 μM and 60 μM) for 24 hours, and the relative wound closure rates were compared to those of blank control cells (Figure 9A). Contrasted with the blank control group, NOB significantly inhibited the migration of B-CPAP cells, but not concentration-dependently (Figure 9B). In sum, NOB curbed the proliferation and migration phenotypes of PTC cells significantly, compared with the control group. Cell proliferation was inhibited by NOB at a concentration-dependent level, but cell migration was not.

The PI3K/AKT Pathway Was Involved in the Inhibition of PTC by NOB

According to KEGG enrichment analysis, NOB suppressed tumor growth, most potentially *via* interfering with PI3K/AKT signal-

ling in PTC. To verify the predicted results of network pharmacology, we determined the protein expression levels of PI3K, P-PI3K, AKT and P-AKT in PTC cells treated with different concentrations of NOB by western blotting. As shown in Figure 9C, target proteins associated with PI3K/AKT signalling were downregulated.

Discussion

The incidence of papillary thyroid carcinoma continues to rise with the upgrading of detection technology¹. Although the prognosis is good, 40-90% of patients are prone to central lymph node metastasis³⁷, and 3-15% of patients will develop distant metastasis³⁸.

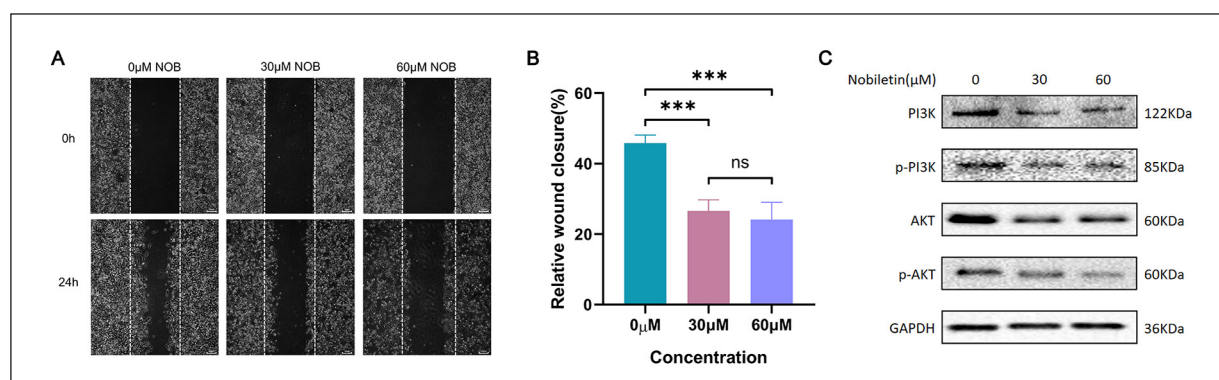


Figure 9. NOB inhibited the migration ability of PTC cells, with down regulation of PI3K, P-PI3K, AKT and P-AKT expression. **A**, Photographs of wound healing taken under the microscope (the scale bar: 20 μm). **B**, Statistical analyses of relative wound closure rate among NOB experimental groups and blank control groups. **C**, An analysis of NOB-induced PI3K/AKT pathway proteins was performed by Western blot, using *GAPDH* for loading control.

Furthermore, relapse occurs in up to 10% of patients after standard treatment³⁹. Data from a large case-control study suggest that lymph node metastases and incomplete surgical resection are the two main attributions for higher mortality⁴⁰. Therefore, at a time when surgery is the main treatment for thyroid cancer, it is essential to improve the clinical medical treatment methods and relieve the suffering of patients. With the effective validation of *in vitro* and *in vivo* models, the anticancer potential of natural products, especially those derived from traditional Chinese medicine, is gradually being recognized by researchers^{41,42}. As a promising avenue of contemporary drug discovery, network pharmacology highlights the better utility of multi-targeted drugs and the network characteristics of intervening diseases^{43,44}.

In this research, we explored how the natural product NOB inhibits PTC with the application of network pharmacology, molecular docking simulation techniques and papillary thyroid cancer cell model. Under the retrieval of existing reports, this is the first time to explore the mechanism of NOB inhibition of PTC through bioinformatics technology and cell experiments. Experiments performed *in vitro* revealed that NOB curbed the proliferation and migration phenotypes of the PTC cell line compared with the control group. It was concentration-dependent that NOB inhibited proliferation but not migration.

Founded on further analysis of the initial predicted targets, we identified three core targets *via* different algorithms, which were *TNF*, *TP53*, and *EGFR*. And this was verified in molecular docking. Tumor necrosis factor (*TNF*), also known as *TNF-alpha* or *TNFSF2*, is a multifunctional proinflammatory cytokine that belongs to the tumor necrosis factor superfamily and plays a dual role in the intervention of cancers which relies upon the involvement of specific cell types and local concentration of *TNF*⁴⁵. A meta-analysis⁴⁶ collecting 29 writings demonstrated that the level of *TNF-α* in serum and the ratio of *TNF-α* immunoreactivity in tissues for thyroid carcinoma were significantly higher in contrast with those in control. NIS's downregulation affects iodine intake and the treatment of radioactive iodine, resulting in a poor prognosis for thyroid cancer patients⁴⁷. And NIS expression can be negatively modulated by *TNF-α*⁴⁸. As a tumor suppressor and a potent cancer barrier, tumor protein *p53* (*TP53*) suppresses tumor growth and induces apoptosis

in many tumors. There is a link between codon 72 polymorphism in the *TP53* gene and thyroid cancer susceptibility⁴⁹. Mutations in *TP53* are involved in thyroid tumor dedifferentiation and progression, causing poorly differentiated thyroid carcinoma (PDTC) and ATC⁵⁰. Dysregulated protein kinase activity contributes to many diseases, including cancer, making the protein kinase family one of the most important drug targets of the 21st century⁵¹. Epidermal growth factor receptor (*EGFR*), a transmembrane glycoprotein that is a member of the protein kinase superfamily, is one of the most common drug targets for FDA-approved drugs. A significant increase in *EGFR* expression was associated with aggressiveness in PTC⁵², and proliferation and migration of PTC cells were inhibited by *EGFR* inhibition⁵³. A dose-expansion study⁵⁴ found that lifirafenib (a novel RAF family kinase inhibitor and *EGFR* inhibitor) had an acceptable risk-benefit profile and antitumor effects on patients with B-RAF^{V600E} PTC.

As we all know, BRAF and RAS mutations are mainly responsible for PTC⁵⁵. And *RAS* activated PI3K/AKT signal pathway in thyroid cancer and had significant associations with AKT phosphorylation⁵⁶. Studies⁵⁷⁻⁶⁰ have shown that the activation of PI3K/AKT signalling was linked to proliferation and migration in PTC cells. NOB was found to exert a tumor-suppressing effect on PTC *via* the PI3K/AKT pathway according to our KEGG enrichment analysis, and this was demonstrated experimentally. Thus, NOB may curb B-CPAP cell proliferation and migration *via* PI3K/AKT signalling.

Conclusions

This research predicted the core targets and key signalling pathways of NOB intervention in PTC, utilizing network pharmacology, molecular docking, and other bioinformatics tools. In cell experiments, it was verified that NOB inhibited PTC proliferation and migration through PI3K/AKT signalling. In summary, for the first time, our study shows an inhibitory effect of NOB on PTC and explores its mechanism.

Conflict of Interest

The Authors declare that they have no conflict of interests.

Acknowledgments

The team should thank a computer professional friend who helped the team fix the difficult scripting problem during the run of the R software.

Authors' Contribution

G.J. and D.Q. contributed to the design of the study. D.Q., W.H., L.Q., and D.W. helped collect data and debug the program. The statistical analysis was carried out by D.Q., L.Q. and Y.Q.

Funding

A total of three projects funded the research, including Senmei China Diabetes Research Fund of China International Medical Foundation (Z-2017-26-1902), Fund Program for the Scientific Activities of Selected Returned Overseas Professionals in Shanxi Province (2020-188), Fund Program for the Scientific Activities of Selected Returned Overseas Professionals in Shanxi Province (20200041).

ORCID ID

Qiuqing Du: 0000-0002-2855-6209.

Ruhao Zhou: 0000-0001-5094-7997.

Jianjin Guo: 0000-0003-4160-4364.

References

- Sugitani I, Ito Y, Takeuchi D, Nakayama H, Masaki C, Shindo H, Teshima M, Horiguchi K, Yoshida Y, Kanai T, Hirokawa M, Hames KY, Tabei I, Miyauchi A. Indications and Strategy for Active Surveillance of Adult Low-Risk Papillary Thyroid Microcarcinoma: Consensus Statements from the Japan Association of Endocrine Surgery Task Force on Management for Papillary Thyroid Microcarcinoma. *Thyroid* 2021; 31: 183-192.
- Feng JW, Hong LZ, Wang F, Wu WX, Hu J, Liu SY, Jiang Y, Ye J. A Nomogram Based on Clinical and Ultrasound Characteristics to Predict Central Lymph Node Metastasis of Papillary Thyroid Carcinoma. *Front Endocrinol (Lausanne)* 2021; 12: 666315.
- Filetti S, Durante C, Hartl D, Leboulleux S, Locati LD, Newbold K, Papotti MG, Berruti A, ESMO Guidelines Committee. Electronic address: clinicalguidelines@esmo.org. Thyroid cancer: ESMO Clinical Practice Guidelines for diagnosis, treatment and follow-up. *Ann Oncol* 2019; 30: 1856-1883.
- Zhang F, Yu X, Lin Z, Wang X, Gao T, Teng D, Teng W. Using Tumor-Infiltrating Immune Cells and a ceRNA Network Model to Construct a Prognostic Analysis Model of Thyroid Carcinoma. *Front Oncol* 2021; 11: 658165.
- Guo M, Chen Z, Li Y, Li S, Shen F, Gan X, Feng J, Cai W, Liu Q, Xu B. Tumor Mutation Burden Predicts Relapse in Papillary Thyroid Carcinoma With Changes in Genes and Immune Microenvironment. *Front Endocrinol (Lausanne)* 2021; 12: 674616.
- Fugazzola L, Elisei R, Fuhrer D, Jarzab B, Leboulleux S, Newbold K, Smit J. 2019 European Thyroid Association Guidelines for the Treatment and Follow-Up of Advanced Radioiodine-Refractory Thyroid Cancer. *Eur Thyroid J* 2019; 8: 227-245.
- Su Y, Cheng S, Qian J, Zhang M, Li T, Zhang Y, Diao C, Zhang L, Cheng R. Case Report: Anlotinib Therapy in a Patient With Recurrent and Metastatic RAIR-DTC Harboring Coexistent TERT Promoter and BRAF(V600E) Mutations. *Front Oncol* 2021; 11: 626076.
- Lever J, Brkljaca R, Kraft G, Urban S. Natural Products of Marine Macroalgae from South Eastern Australia, with Emphasis on the Port Phillip Bay and Heads Regions of Victoria. *Mar Drugs* 2020; 18: 142.
- Deng LJ, Qi M, Li N, Lei YH, Zhang DM, Chen JX. Natural products and their derivatives: Promising modulators of tumor immunotherapy. *J Leukoc Biol* 2020; 108: 493-508.
- Ru J, Li P, Wang J, Zhou W, Li B, Huang C, Li P, Guo Z, Tao W, Yang Y, Xu X, Li Y, Wang Y, Yang L. TCMSP: a database of systems pharmacology for drug discovery from herbal medicines. *J Cheminform* 2014; 6: 13.
- Hosokawa Y, Hosokawa I, Ozaki K, Matsuo T. Nobiletin Inhibits Inflammatory Reaction in Interleukin-1beta-Stimulated Human Periodontal Ligament Cells. *Pharmaceutics* 2021; 7: 667.
- Gandhi GR, Vasconcelos ABS, Wu DT, Li HB, Antony PJ, Li H, Geng F, Gurgel RQ, Narain N, Gan RY. Citrus Flavonoids as Promising Phytochemicals Targeting Diabetes and Related Complications: A Systematic Review of In Vitro and In Vivo Studies. *Nutrients* 2020; 12: 2907.
- Sp N, Kang DY, Lee JM, Jang KJ. Mechanistic Insights of Anti-Immune Evasion by Nobiletin through Regulating miR-197/STAT3/PD-L1 Signaling in Non-Small Cell Lung Cancer (NSCLC) Cells. *Int J Mol Sci* 2021; 22: 9843.
- Wei D, Zhang G, Zhu Z, Zheng Y, Yan F, Pan C, Wang Z, Li X, Wang F, Meng P, Zheng W, Yan Z, Zhai D, Lu Z, Yuan J. Nobiletin Inhibits Cell Viability via the SRC/AKT/STAT3/YY1AP1 Pathway in Human Renal Carcinoma Cells. *Front Pharmacol* 2019; 10: 690.
- Zhang R, Chen J, Mao L, Guo Y, Hao Y, Deng Y, Han X, Li Q, Liao W, Yuan M. Nobiletin Triggers Reactive Oxygen Species-Mediated Pyroptosis through Regulating Autophagy in Ovarian Cancer Cells. *J Agric Food Chem* 2020; 68: 1326-1336.
- Huang J, Chang Z, Lu Q, Chen X, Najafi M. Nobiletin as an inducer of programmed cell death in cancer: a review. *Apoptosis* 2022; 27: 297-310.

- 17) Feng SL, Tian Y, Huo S, Qu B, Liu RM, Xu P, Li YZ, Xie Y. Nobiletin potentiates paclitaxel anticancer efficacy in A549/T xenograft model: Pharmacokinetic and pharmacological study. *Phyto-medicine* 2020; 67: 153141.
- 18) Zhu G, Zhang J, Yang Y, Zhang H, Jin W, Su F, Liang J, Wang K, Zhang J, Chen C. The Key Target and Molecular Mechanism of the Volatile Component of *Scutellaria baicalensis* Georgi in Acute Lung Injury Based on Network Pharmacology. *Front Pharmacol* 2021; 12: 650780.
- 19) Nguyen NT, Nguyen TH, Pham TNH, Huy NT, Bay MV, Pham MQ, Nam PC, Vu VV, Ngo ST. Autodock Vina Adopts More Accurate Binding Poses but Autodock4 Forms Better Binding Affinity. *J Chem Inf Model* 2020; 60: 204-211.
- 20) Guo J, Chen J, Ren W, Zhu Y, Zhao Q, Zhang K, Su D, Qiu C, Zhang W, Li K. Citrus flavone tangeretin is a potential insulin sensitizer targeting hepatocytes through suppressing MEK-ERK1/2 pathway. *Biochem Biophys Res Commun* 2020; 529: 277-282.
- 21) Daina A, Michielin O, Zoete V. SwissTargetPrediction: updated data and new features for efficient prediction of protein targets of small molecules. *Nucleic Acids Res* 2019; 47: W357-W64.
- 22) Yao ZJ, Dong J, Che YJ, Zhu MF, Wen M, Wang NN, Wang S, Lu AP, Cao DS. TargetNet: a web service for predicting potential drug-target interaction profiling via multi-target SAR models. *J Comput Aided Mol Des* 2016; 30: 413-424.
- 23) Safran M, Rosen N, Twik M, BarShir R, Stein TI, Dahary D, Fishilevich S, Lancet D. *Practical Guide to Life Science Databases*. Springer Singapore, 2021.
- 24) Whirl-Carrillo M, Huddart R, Gong L, Sangkuhl K, Thorn CF, Whaley R, Klein TE. An Evidence-Based Framework for Evaluating Pharmacogenomics Knowledge for Personalized Medicine. *Clin Pharmacol Ther* 2021; 110: 563-572.
- 25) Amberger JS, Bocchini CA, Scott AF, Hamosh A. OMIM.org: leveraging knowledge across phenotype-gene relationships. *Nucleic Acids Res* 2019; 47: D1038-D1043.
- 26) Pinero J, Ramirez-Anguaita JM, Sauch-Pitarch J, Ronzano F, Centeno E, Sanz F, Furlong LI. The DisGeNET knowledge platform for disease genomics: 2019 update. *Nucleic Acids Res* 2020; 48: D845-D855.
- 27) Sherman BT, Hao M, Qiu J, Jiao X, Baseler MW, Lane HC, Imamichi T, Chang W. DAVID: a web server for functional enrichment analysis and functional annotation of gene lists (2021 update). *Nucleic Acids Res* 2022; 50: W216-W221.
- 28) Shannon P, Markiel A, Ozier O, Baliga NS, Wang JT, Ramage D, Amin N, Schwikowski B, Ideker T. Cytoscape: a software environment for integrated models of biomolecular interaction networks. *Genome Res* 2003; 13: 2498-2504.
- 29) Chen H, Lai M, Zhang T, Chen Y, Tong L, Zhu S, Zhou Y, Ren X, Ding J, Xie H, Lu X, Ding K. Conformational Constrained 4-(1-Sulfonyl-3-indolyl)-2-phenylaminopyrimidine Derivatives as New Fourth-Generation Epidermal Growth Factor Receptor Inhibitors Targeting T790M/C797S Mutations. *J Med Chem* 2022; 65: 6840-6858.
- 30) Degtjarik O, Golovenko D, Diskin-Posner Y, Abrahmsen L, Rozenberg H, Shakked Z. Structural basis of reactivation of oncogenic p53 mutants by a small molecule: methylene quinuclidinone (MQ). *Nat Commun* 2021; 12: 7057.
- 31) He MM, Smith AS, Oslob JD, Flanagan WM, Braisted AC, Whitty A, Cancilla MT, Wang J, Lugovskoy AA, Yoburn JC, Fung AD, Farrington G, Eldredge JK, Day ES, Cruz LA, Cachero TG, Miller SK, Friedman JE, Choong IC, Cunningham BC. Small-molecule inhibition of TNF-alpha. *Science* 2005; 310: 1022-1025.
- 32) Jimenez J, Doerr S, Martinez-Rosell G, Rose AS, De Fabritiis G. DeepSite: protein-binding site predictor using 3D-convolutional neural networks. *Bioinformatics* 2017; 33: 3036-3042.
- 33) Eberhardt J, Santos-Martins D, Tillack AF, Forli S. AutoDock Vina 1.2.0: New Docking Methods, Expanded Force Field, and Python Bindings. *J Chem Inf Model* 2021; 61: 3891-3898.
- 34) Adasme MF, Linnemann KL, Bolz SN, Kaiser F, Salentin S, Haupt VJ, Schroeder M. PLIP 2021: expanding the scope of the protein-ligand interaction profiler to DNA and RNA. *Nucleic Acids Res* 2021; 49: W530-W534.
- 35) Schrodinger, LLC. *The PyMOL Molecular Graphics System, Version 2.6.0*. 2015.
- 36) Wang K, Qian R, Li H, Wang C, Ding Y, Gao Z. Interpreting the Pharmacological Mechanisms of Sho-saiko-to on Thyroid Carcinoma through Combining Network Pharmacology and Experimental Evaluation. *ACS Omega* 2022; 7: 11166-11176.
- 37) Wu Y, Rao K, Liu J, Han C, Gong L, Chong Y, Liu Z, Xu X. Machine Learning Algorithms for the Prediction of Central Lymph Node Metastasis in Patients With Papillary Thyroid Cancer. *Front Endocrinol (Lausanne)* 2020; 11: 577537.
- 38) Albano D, Panarotto MB, Durmo R, Rodella C, Bertagna F, Giubbini R. Clinical and prognostic role of detection timing of distant metastases in patients with differentiated thyroid cancer. *Endocrine* 2019; 63: 79-86.
- 39) Pamedytyte D, Simanaviciene V, Dauksiene D, Leipute E, Zvirbliene A, Sarauskas V, Dauksa A, Verkauskiene R, Zilaitiene B. Association of MicroRNA Expression and BRAF(V600E) Mutation with Recurrence of Thyroid Cancer. *Biomolecules* 2020; 10: 625.
- 40) Wu T, Zhang DL, Wang JM, Jiang JY, Du X, Zeng XY, Du ZX. TRIM29 inhibits miR-873-5P biogenesis via CYTOR to upregulate fibronectin 1 and promotes invasion of papillary thyroid cancer cells. *Cell Death Dis* 2020; 11: 813.
- 41) Zhu XY, Guo DW, Lao QC, Xu YQ, Meng ZK, Xia B, Yang H, Li CQ, Li P. Sensitization and syner-

- gistic anti-cancer effects of Furanodiene identified in zebrafish models. *Sci Rep* 2019; 9: 4541.
- 42) Cui H, Bashar MAE, Rady I, El-Naggar HA, Abd El-Maoula LM, Mehany ABM. Antiproliferative Activity, Proapoptotic Effect, and Cell Cycle Arrest in Human Cancer Cells of Some Marine Natural Product Extract. *Oxid Med Cell Longev* 2020; 2020: 7948705.
 - 43) Shen Y, Zhang B, Pang X, Yang R, Chen M, Zhao J, Wang J, Wang Z, Yu Z, Wang Y, Li L, Liu A, Du G. Network Pharmacology-Based Analysis of Xiao-Xu-Ming Decoction on the Treatment of Alzheimer's Disease. *Front Pharmacol* 2020; 11: 595254.
 - 44) Wang X, Xin B, Tan W, Xu Z, Li K, Li F, Zhong W, Peng S. DeepR2cov: deep representation learning on heterogeneous drug networks to discover anti-inflammatory agents for COVID-19. *Brief Bioinform* 2021; 22: bbab226.
 - 45) Chen AY, Wolchok JD, Bass AR. TNF in the era of immune checkpoint inhibitors: friend or foe? *Nat Rev Rheumatol* 2021; 17: 213-223.
 - 46) Zhao J, Wen J, Wang S, Yao J, Liao L, Dong J. Association between adipokines and thyroid carcinoma: a meta-analysis of case-control studies. *BMC Cancer* 2020; 20: 788.
 - 47) Wang H, Ma Z, Cheng X, Tuo B, Liu X, Li T. Physiological and Pathophysiological Roles of Ion Transporter-Mediated Metabolism in the Thyroid Gland and in Thyroid Cancer. *Onco Targets Ther* 2020; 13: 12427-12441.
 - 48) Faria M, Domingues R, Paixao F, Bugalho MJ, Matos P, Silva AL. TNF α -mediated activation of NF- κ B downregulates sodium-iodide symporter expression in thyroid cells. *PLoS One* 2020; 15: e0228794.
 - 49) Khan MS, Pandith AA, Masoodi SR, Khan SH, Rather TA, Andrabi KI, Mudassar S. Significant association of TP53 Arg72Pro polymorphism in susceptibility to differentiated thyroid cancer. *Cancer Biomark* 2015; 15: 459-465.
 - 50) Haroon Al Rasheed MR, Xu B. Molecular Alterations in Thyroid Carcinoma. *Surg Pathol Clin* 2019; 12: 921-930.
 - 51) Roskoski R, Jr. Properties of FDA-approved small molecule protein kinase inhibitors: A 2021 update. *Pharmacol Res* 2021; 165: 105463.
 - 52) Jankovic J, Tatic S, Bozic V, Zivaljevic V, Cvejic D, Paskas S. Inverse expression of caveolin-1 and EGFR in thyroid cancer patients. *Hum Pathol* 2017; 61: 164-172.
 - 53) Han JY, Guo S, Wei N, Xue R, Li W, Dong G, Li J, Tian X, Chen C, Qiu S, Wang T, Xiao Q, Liu C, Xu J, Chen KS. ciRS-7 Promotes the Proliferation and Migration of Papillary Thyroid Cancer by Negatively Regulating the miR-7/Epidermal Growth Factor Receptor Axis. *Biomed Res Int* 2020; 2020: 9875636.
 - 54) Desai J, Gan H, Barrow C, Jameson M, Atkinson V, Haydon A, Millward M, Begbie S, Brown M, Markman B, Patterson W, Hill A, Horvath L, Nagrial A, Richardson G, Jackson C, Friedlander M, Parente P, Tran B, Wang L, Chen Y, Tang Z, Huang W, Wu J, Zeng D, Luo L, Solomon B. Phase I, Open-Label, Dose-Escalation/Dose-Expansion Study of Lifirafenib (BGB-283), an RAF Family Kinase Inhibitor, in Patients With Solid Tumors. *J Clin Oncol* 2020; 38: 2140-2150.
 - 55) Lewinski A, Adamczewski Z, Zygmunt A, Markuszewski L, Karbownik-Lewinska M, Stasiak M. Correlations between Molecular Landscape and Sonographic Image of Different Variants of Papillary Thyroid Carcinoma. *J Clin Med* 2019; 8: 1916.
 - 56) Zhou C, Yang C, Chong D. E-cadherin expression is associated with susceptibility and clinicopathological characteristics of thyroid cancer: A PRISMA-compliant meta-analysis. *Medicine (Baltimore)* 2019; 98: e16187.
 - 57) Dong X, Akuetteh PDP, Song J, Ni C, Jin C, Li H, Jiang W, Si Y, Zhang X, Zhang Q, Huang G. Major Vault Protein (MVP) Associated With BRAF (V600E) Mutation Is an Immune Microenvironment-Related Biomarker Promoting the Progression of Papillary Thyroid Cancer via MAPK/ERK and PI3K/AKT Pathways. *Front Cell Dev Biol* 2021; 9: 688370.
 - 58) Srivastava A, Kumar A, Giangiobbe S, Bonora E, Hemminki K, Forsti A, Bandapalli OR. Whole Genome Sequencing of Familial Non-Medullary Thyroid Cancer Identifies Germline Alterations in MAPK/ERK and PI3K/AKT Signaling Pathways. *Biomolecules* 2019; 9: 605.
 - 59) Wang Y, Wang C, Fu Z, Zhang S, Chen J. miR-30b-5p inhibits proliferation, invasion, and migration of papillary thyroid cancer by targeting GALNT7 via the EGFR/PI3K/AKT pathway. *Cancer Cell Int* 2021; 21: 618.
 - 60) Zheng Z, Zhou X, Cai Y, Chen E, Zhang X, Wang O, Wang Q, Liu H. TEK4 Promotes Papillary Thyroid Cancer Cell Proliferation, Colony Formation, and Metastasis through Activating PI3K/Akt Pathway. *Endocr Pathol* 2018; 29: 310-316.